© 1999 The Chemical Society of Japan


# Electrochemical Luminescence of $ZnGa_2O_4$ and $ZnGa_2O_4$ : Mn Semiconductor Electrodes. —Emission Mechanism under Cathodic and Anodic Polarization—

**Toshihito Ohtake, Noriyuki Sonoyama, and Tadayoshi Sakata***

Department of Electronic Chemistry, Interdisciplinary Graduate School of Science and Engineering, Tokyo Institute of Technology, 4259 Nagatsuta, Midori-ku, Yokohama 226-8502

(Received April 22, 1999)

Electrochemical luminescence properties and mechanism of $ZnGa_2O_4$ and $ZnGa_2O_4$ : Mn ($ZnGa_2O_4$ doped with Mn) were studied. $ZnGa_2O_4$ disk showed an n-type semiconductor property after reduction in $H_2$ atmosphere. Under cathodic polarization, the emission in a $ZnGa_2O_4$ electrode showed a broad peak at 485 nm in $Na_2S_2O_8$ electrolyte solution. $ZnGa_2O_4$ : Mn exhibited a sharp emission peak at about 500 nm based on $Mn^{2+}$, and a broad peak of $ZnGa_2O_4$ was also observed with increasing the cathodic bias. Under anodic polarization in $Na_2SO_4$ electrolyte, electrochemical luminescence was observed from the $ZnGa_2O_4$ electrode surface at +12.5 V (vs. Ag/AgCl) with two emission peaks at about 500 and 700 nm. The emission mechanism based on avalanche breakdown and impact excitation of emission centers by injected electrons is proposed. By adding $K_4[Fe(CN)_6]$, KI, and KBr as reducing agents to the $Na_2SO_4$ electrolyte, the emission intensity was increased in the order KBr < KI < $K_4[Fe(CN)_6]$. Temperature dependence of the emission intensity suggests that electron transfer at the $ZnGa_2O_4$/electrolyte interface occurs equi-energetically from the occupied energy level of each reducing agent to the conduction band of $ZnGa_2O_4$.

$ZnGa_2O_4$ phosphor has been investigated for its excellent properties in cathodoluminescent material.[1—3] There is growing interest in $ZnGa_2O_4$ and $ZnGa_2O_4$ : Mn ($ZnGa_2O_4$ doped with Mn) as low-voltage cathodoluminescent phosphors for field emission displays (FED)[4] and vacuum fluorescent displays (VFDs).[5] FED is a new kind of vacuum flat cathode ray tube. Due to the attractive advantage of FED, it is a good candidate for replacing the conventional cathode ray tube (CRT) in flat panel display. $ZnGa_2O_4$ is a possible alternative to the ZnS-based low-voltage cathodoluminescence phosphors presently used in VFDs. The high stability of the oxide phosphors in vacuum under electron bombardment offers advantages over the commonly used sulfide phosphors.[6,7]

The luminescence of $ZnGa_2O_4$ : Mn has been studied by several groups.[8—10] Its green emission is peaked at 500 nm.[11] Activation with $Mn^{2+}$ causes a luminescence of $^4T_1$—$^6A_1$ transition between 3d electrons within the $Mn^{2+}$ ion that is optically forbidden. The $Mn^{2+}$ ion is assumed to replace the Zn atoms of the $ZnGa_2O_4$ host lattice, because of the same valency.[12]

$ZnGa_2O_4$ is a binary oxide consisting of ZnO and $Ga_2O_3$ that crystallizes in spinel structure.[8] The unit cell of spinels is represented by formula of $AB_2O_4$. The $Zn^{2+}$ ions occupy the tetrahedrally coordinated A site and the $Ga^{3+}$ ions occupy the octahedrally coordinated B sites.[13,14] The green emission of $ZnGa_2O_4$ : Mn is considered to be caused by $Mn^{2+}$ ions that replaced the $Zn^{2+}$ ions in the tetrahedrally coordinated A site.

Although the crystal structure and cathodoluminescence of $ZnGa_2O_4$ is known, its property and electrochemical luminescence are not known, as far as we know. Concentrations of electrons and holes in a semiconductor can be easily controlled by injecting carriers externally or doping impurity atoms. It is particularly easy for semiconductor electrodes. For a semiconductor electrode it is also easy to generate electrochemical luminescence (ECL) by imposing a few volts to the electrode. For the electrochemical luminescence of semiconductor electrodes, high voltage and high vacuum like cathodoluminescence is not needed. If $ZnGa_2O_4$ and $ZnGa_2O_4$ : Mn can be used as a semiconductor electrode, one can obtain information about the emission mechanism from a viewpoint of photo electrochemistry, and can expect to develop new applications.[15] In this study, an application for a semiconductor electrode was attempted by preparing sintered disks of $ZnGa_2O_4$ and $ZnGa_2O_4$ : Mn phosphors. Electrochemical luminescence was observed like cathodoluminescence by imposing cathodic bias to the $ZnGa_2O_4$ in $Na_2S_2O_8$ electrolyte solution, and a new spectrum was obtained under strong anodic polarization up to +12.5 V (vs. Ag/AgCl). In a previous study, we briefly reported electrochemical luminescence of the $ZnGa_2O_4$ electrode.[16] In the present manuscript, we would like to report current–voltage property as well as the emission spectra, and to discuss the electrochemical luminescence mechanism for $ZnGa_2O_4$ and $ZnGa_2O_4$ : Mn electrodes in detail.

## Experimental

$ZnGa_2O_4$ phosphor was prepared by solid state reaction with

mixing ZnO (Furuuchi Chemical 99.999%) and $Ga_2O_3$ (Furuuchi Chemical 99.9%) in 1 : 1 molar ratio. $ZnGa_2O_4$ : Mn phosphor was prepared by adding 0.5% MnO (Aldrich 99.99%) to ZnO and $Ga_2O_3$ mixed powder. The mixed powder was ball-milled in methanol and, after being dried up, pre-sintered in air at 1100 °C for 10 h in alumina crucibles. After grinding and mixing by ball-mill in methanol, the sintered powder was dried and pressed into 20 mm diameter disks. The pressed disks were sintered at 1400 °C for 10 h in air, and were reduced under $H_2$ stream at 600 °C for 10 h. The disks were connected with a copper wire after making an ohmic contact with In–Ga alloy. The back side of the disk was coated with an epoxy resin.

Measurements were carried out under potentiostatic control in a conventional cell with a platinum counter electrode and a Ag/AgCl reference electrode. The luminescence was measured by applying voltage with potentiostat (Hokuto Denko Ltd., HA-501 or HA-3001). The emission spectra were measured by a spectrofluorometer (SPEX Industries Inc., Fluoro Max™). Photomultiplier tube sensitivity was not corrected.

## Results and Discussion

**Semiconductor Property of $ZnGa_2O_4$ Electrode.** Sintered disks prepared by sintering $ZnGa_2O_4$ powder in air were not conductor but insulator. After reduction under $H_2$ stream at 600 °C for 10 h, the sintered disks became conductive. The resistivity was about 270 Ω cm and the band gap of $ZnGa_2O_4$ was evaluated to be 4.6 eV from $(Ahv)^2$ vs. $hv$ plot. Here $A$ and $hv$ represent the absorbance and photon energy, respectively. This value agreed with the reported band gap of 4.4 eV.[5] Figure 1 shows a current–voltage curve of a sintered $ZnGa_2O_4$ electrode in 0.5 M $Na_2SO_4$ solution (1 M = 1 mol $dm^{-3}$) measured at a sweep rate of 50 mV $s^{-1}$. When the electrode potential was swept from rest potential to cathodic potential, cathodic current was observed to flow at about −1.0 V. When the $ZnGa_2O_4$ electrode was polarized at about −4.0 V, the cathodic current reached about 120 mA $cm^{-2}$ and $H_2$ evolution was observed on the electrode surface because of electrochemical reduction of $H_2O$. Under anodic polarization, no anodic current was observed even to about +2.0 V. The rectification property indicates that the $ZnGa_2O_4$ electrode is an n-type semiconductor. The $ZnGa_2O_4$ : Mn electrode also exhibited similar electrochemical behavior.

**Electrochemical Luminescence under Cathodic Polarization.** Electrochemical luminescence was observed for the $ZnGa_2O_4$ electrode under cathodic polarization in electrolyte solution containing $Na_2S_2O_8$, as shown in Fig. 2. The electrochemical luminescence began to be observed at about −1.5 V. The emission intensity increased with increasing the cathodic bias. The emission spectra exhibited a broad peak at 485 nm, extending from 350 to 700 nm. It is reported that the cathodoluminescence spectra of $ZnGa_2O_4$ indicate a peak at 470 nm[17,18] and the photoluminescence spectra exhibit a peak at 480 nm.[5] Since the electrochemical luminescence spectra of Fig. 2 agree well with these reported spectra, it is ascribed to luminescence from $ZnGa_2O_4$. It is noted that the emission of $ZnGa_2O_4$ could be observed by applying a small cathodic bias of several volts. By increasing the cathodic bias, degradation of the electrode progressed with $H_2$ evolution, resulting in a color change of the electrode surface.

Figure 3 shows electrochemical luminescence of a $ZnGa_2O_4$ : Mn electrode. The electrochemical luminescence spectra indicated a sharp peak at about 500 nm at potentials below −1.3 V, and the emission intensity increased with increasing the cathodic polarization as shown in Fig. 3(a). Besides the 500 nm, emission a weak luminescence was observed at about 680 nm. $ZnGa_2O_4$ : Mn has been reported to generate green emission at 506 nm based on $Mn^{2+}$ when excited at 254 nm.[9] Red emission based on $Mn^{4+}$ at 666 nm has also been reported.[10] From these results, it is concluded that the emission at about 500 nm is based on $Mn^{2+}$, and that the very weak emission at 680 nm arises from $Mn^{4+}$. It is thought that $Mn^{4+}$ ions were formed by the oxidation of $Mn^{2+}$ when the $ZnGa_2O_4$ : Mn was sintered in air. With increasing the cathodic bias, sharp emission at about 500 nm changed to broad emission at 350—750 nm, as shown in Fig. 3(b). This broad emission increased in intensity continuously with increasing the cathodic bias. Since the broad emission peaked at about 490 nm resembles the emission spectra in Fig. 2, it is attributed to emission from $ZnGa_2O_4$. Thus the electroluminescence spectra of the $ZnGa_2O_4$ electrode changed from sharp spectra with a peak at about 500 nm to a broad spec-

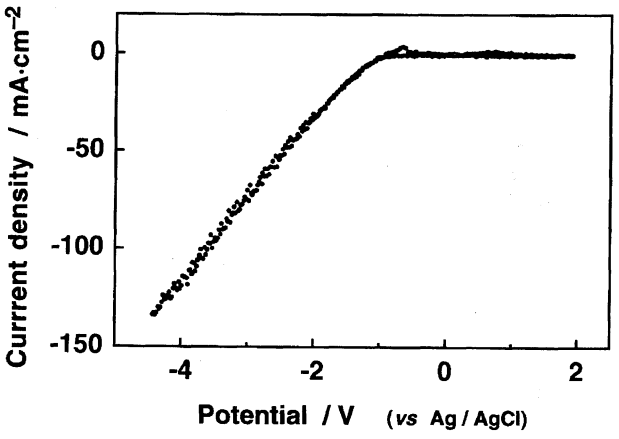


Fig. 1. Current–voltage measurement of $ZnGa_2O_4$ electrode in 0.5 M $Na_2SO_4$ electrolyte.

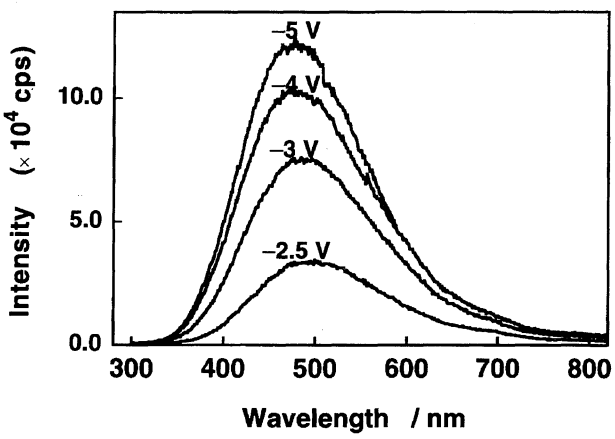


Fig. 2. Emission spectra of $ZnGa_2O_4$ electrode under cathodic bias in 0.5 M $Na_2S_2O_8$ + 2 M NaOH.

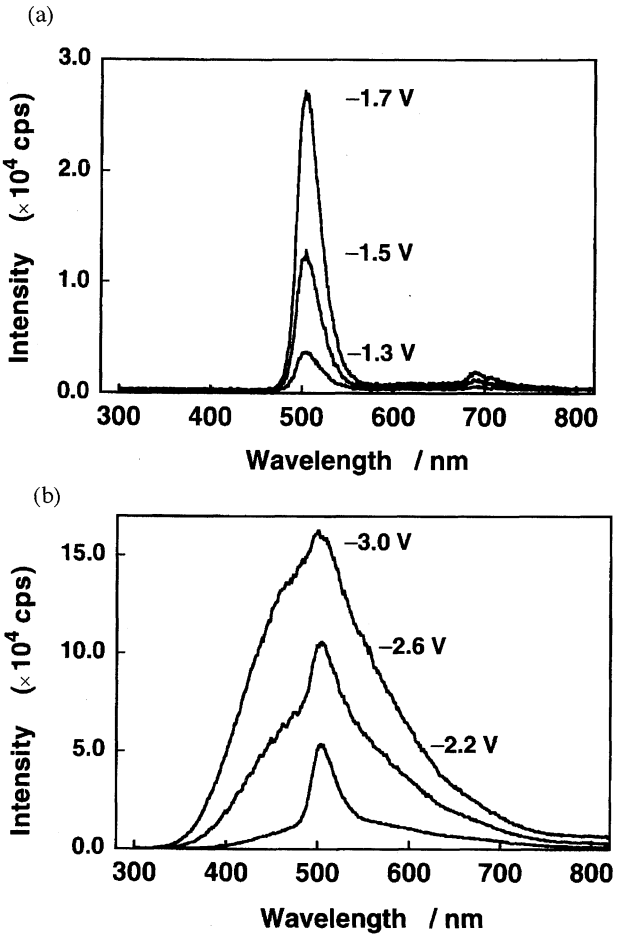


Fig. 3. Emission spectra of $ZnGa_2O_4$ : Mn electrode under cathodic bias in 0.5 M $Na_2S_2O_8$ + 2 M NaOH. (a) Imposed cathodic bias is from −1.3 to −1.7 V. (b) Imposed cathodic bias is from −2.2 to −3.0 V.

tra expanding at 350—750 nm, depending on the electrode potential.

It is known that an n-type semiconductor electrode shows electroluminescence in the presence of $Na_2S_2O_8$, and the luminescence mechanism could be explained as recombination with electrons in the conduction band and holes injected by $S_2O_8^{2-}$ reduction.[19—22] Figure 4 schematically illustrates the electrochemical luminescence mechanism of $ZnGa_2O_4$ and $ZnGa_2O_4$ : Mn electrodes under cathodic polarization in $Na_2S_2O_8$ electrolyte solution. The $SO_4^{-\cdot}$ radical is formed by reduction of $S_2O_8^{2-}$ when the $ZnGa_2O_4$ electrode is polarized cathodically.

$$S_2O_8^{2-} + e^-(\text{C.B.}) \rightarrow SO_4^{-\cdot} + SO_4^{2-} \quad (1)$$

Holes are injected in the valence band of $ZnGa_2O_4$ because the $SO_4^{-\cdot}$ is a strong oxidizing agent.[23]

$$SO_4^{-\cdot} \rightarrow SO_4^{2-} + h^+(\text{V.B.}) \quad (2)$$

The emission of the $ZnGa_2O_4$ electrode is caused by recombination between the electrons in the conduction band and the injected holes in the valence band.

In the case of the $ZnGa_2O_4$ : Mn electrode, it is considered

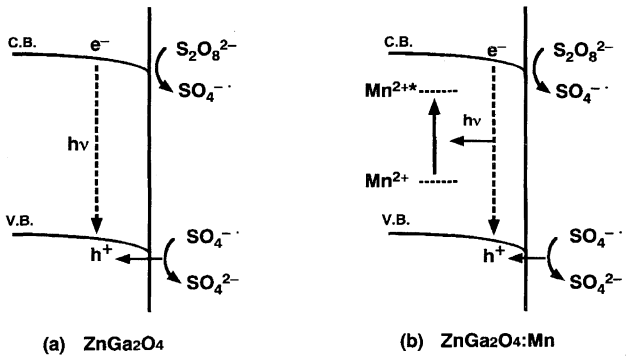


Fig. 4. A schematic mechanism of electrochemical luminescence under cathodic polarization.

that the recombination takes place at the $Mn^{2+}$ site to excite $Mn^{2+}$.

$$Mn^{2+} + e^- + h^+ \rightarrow Mn^{2+*} \quad (3)$$

Here, $Mn^{2+*}$ represents an excited $Mn^{2+}$ ion in the $ZnGa_2O_4$ lattice. As shown in Fig. 3(a), it is considered that such an emission based on $Mn^{2+}$ is observed by imposing cathodic voltage until −1.7 V.

With increasing the cathodic voltages further, the emission based on $ZnGa_2O_4$ is observed together with emission based on $Mn^{2+}$, as shown in Fig. 3(b). For the $ZnGa_2O_4$ : Mn electrode, cathodic current is increased with increasing the cathodic polarization, as in the case of the $ZnGa_2O_4$ electrode in Fig. 1. Accompanied by the increased cathodic current, $S_2O_8^{2-}$ reduction of Eq. 1 proceeds efficiently, and results in efficient hole injection of Eq. 2. Therefore, emission based on the recombination of electrons and holes in $ZnGa_2O_4$ occurs besides that based on $Mn^{2+}$, i.e. Eq. 3 with increasing the cathodic current. This might be a reason why increased cathodic potential generates broad emission based on $ZnGa_2O_4$, even for the $ZnGa_2O_4$ : Mn electrode as shown in Fig. 3(b).

**Electrochemical Luminescence under Anodic Polarization.** When the $ZnGa_2O_4$ and $ZnGa_2O_4$ : Mn electrode was polarized anodically, no electroluminescence was observed until about +12.0 V. However, strong luminescence was observed when it was polarized up to +12.5 V. Figure 5 shows the dependence of the electrochemical luminescence on the current density, which was controlled galvanostatically. In the case of the $ZnGa_2O_4$ electrode as shown in Fig. 5a, the emission was observed for current densities $\geq 3$ mA $cm^{-2}$. The emission spectrum shows two peaks at 503 nm and at about 700 nm. In the case of the $ZnGa_2O_4$ : Mn electrode as shown in Fig. 5(b), very strong emission was observed at about 500 nm and emission peak about 700 nm was very weak. The emission intensity of the $ZnGa_2O_4$ : Mn electrode was about ten-times stronger than that of the $ZnGa_2O_4$ electrode. Both emission intensities increased remarkably with increasing the anodic current density. Because the anodic current indicates oxidation on the electrode surface, electrons injected by the reaction seem to cause the luminescence. Furthermore, the luminescence spectra in Fig. 5(a) are quite different from those under cathodic polarization in

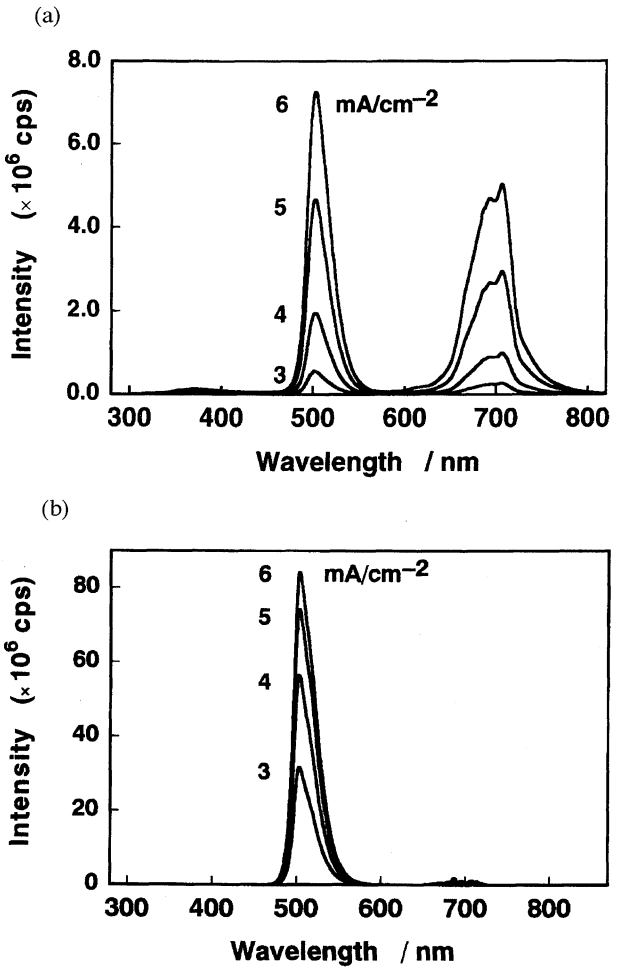


Fig. 5. Emission spectra under anodic bias in 0.5 M $Na_2SO_4$ electrolyte. (a) $ZnGa_2O_4$ electrode. (b) $ZnGa_2O_4$ : Mn electrode.

Fig. 2. This suggests that the luminescence mechanism at the anodic polarization is quite different from the case of cathodic polarization.

In order to investigate the electrochemical luminescence mechanism of $ZnGa_2O_4$, current–voltage measurements of the $ZnGa_2O_4$ electrode were carried out in 0.5 M $Na_2SO_4$. Only a small saturation current was observed under low anodic polarization. However, an abrupt rise of the anodic current was observed when the electrode potential reached about +12.5 V. This abrupt rise of the anodic current is interpreted as breakdown of the depletion layer in the $ZnGa_2O_4$ electrode. Although the electrochemical luminescence was not observed at a low electrode potential, it was observed at about +12.5 V with an abrupt rise in the anodic current. The abrupt rise in the anodic current in the n-type $ZnGa_2O_4$ electrode suggests that it was caused by breakdown of the depletion layer at the $ZnGa_2O_4$/electrolyte interface, as known for Zener effect (tunnel effect)[24,25] and avalanche breakdown[26,27] are known well as the breakdown mechanism of the p–n junction in semiconductors. In the Zener effect, electrons pass through the barrier by quantum-mechanical tunneling when its thickness is very thin, while in avalanche breakdown electrons run through the barrier by impact ionization colliding with the crystal lattice when the barrier is in a strong electric field. Gautron et al. observed emission from an n-type ZnSe electrode under anodic polarization,[28] and regarded the emission based on electron transfer to conduction band in ZnSe by tunneling.[29] On the other hand, Tranchart et al. observed an anodic current under anodic bias by using an n-type GaAs electrode, and explained the anodic current by avalanche breakdown.[26] However, the breakdown mechanism and its relation with electrochemical luminescence under anodic polarization is not clear.

As shown at temperature dependence of current–voltage curves in Fig. 6, the breakdown potential increases with increasing temperature. It is known that in the case of breakdown by tunneling effect, the breakdown voltage becomes small with increasing temperature, while it becomes large with increasing temperature in the case of avalanche breakdown.[30] The result in Fig. 6 indicates that the breakdown mechanism in the case of $ZnGa_2O_4$ is avalanche breakdown. The temperature dependence of avalanche breakdown is explained by electron scattering caused by vigorous lattice vibration with increasing temperature. In the case of

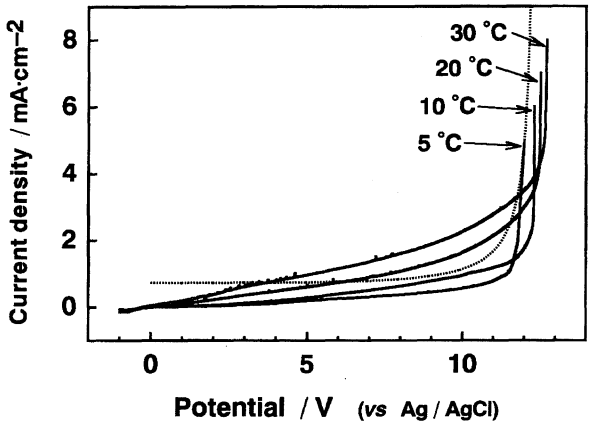


Fig. 6. Temperature dependence of current-voltage property in $ZnGa_2O_4$ electrode. Broken line shows a theoretical curve at 20 °C calculated by Eq. 4.

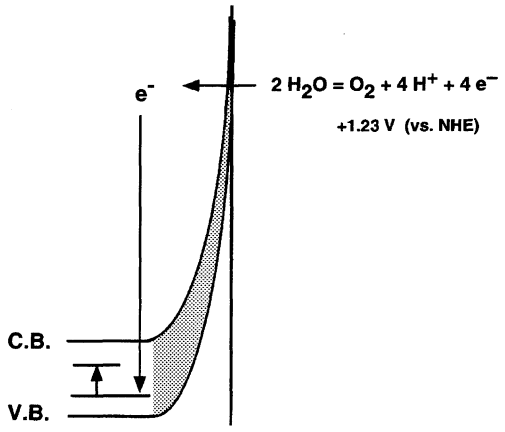


Fig. 7. A schematic mechanism of electrochemical luminescence under anodic polarization in the absence of reducing agent.

avalanche breakdown, the breakdown current is explained experimentally by the following equation.[30]

$$i = i_0 M = i_0 \frac{1}{1 - \left(\frac{V}{V_B}\right)^n}. \quad (4)$$

Here, $i_0$ is the saturation current and $V_B$ is the breakdown voltage. Equation 4 gives

$$\log\left(1 - \frac{i_0}{i}\right) = n(\log V - \log V_B). \quad (5)$$

As can be seen in Eq. 5, the slope of $\log(1-\frac{i_0}{i})$ vs. $\log V$ plots is equal to $n$; $n = 4.8$ was obtained from the slope of $\log(1-\frac{i_0}{i})$ vs. $\log V$ plots. The broken line in Fig. 6 shows a theoretical current-voltage curve simulated by using Eq. 5 with $n = 4.8$, $V_B = 12.4$ V and $i_0 = 0.7299$ mA cm$^{-2}$. Although the agreement between theory and experimental curves is not very good, the simulated curve represents well the characteristic features of the experimental current–voltage curves.

Figure 7 schematically illustrates the mechanism of the electrochemical luminescence of the $ZnGa_2O_4$ electrode under anodic polarization. The above results demonstrate that the abrupt rise of the anodic current at about +12.5 V represents avalanche breakdown, in which electrons are injected to the conduction band of the $ZnGa_2O_4$ electrode from water molecules on the electrode surface. Since injected electrons are accelerated at a strong electric field of the depletion layer under strong anodic polarization, they obtain a large kinetic energy in the electric field. Thus, electrochemical luminescence would be generated by impact excitation of the luminescence centers of the $ZnGa_2O_4$ by these energetic injected electrons. This impact excitation mechanism is different from the mechanism of the electrochemical luminescence of the $ZnGa_2O_4$ electrode under cathodic polarization in the presence of $Na_2S_2O_8$.

Although the emission spectra of the $ZnGa_2O_4$ electrode in Fig. 5(a) have not yet been reported, it resembles the emission spectra of ZnO. When high purity ZnO powder is sintered in a reduction atmosphere, it shows green emission at about 510 nm by exciting it at 350 nm.[31] The luminescence center of the green emission is considered to be Zn atoms in the ZnO lattice. Since the emission spectra of the $ZnGa_2O_4$ electrode resembles this green emission of ZnO, its emission center is considered to be the Zn atom in the $ZnGa_2O_4$ that has been produced by hydrogen reduction. Barthou et al. observed the emission spectra of $Zn_2SiO_4$ at 670—740 nm.[32] They ascribed it to luminescence from the oxygen defect in the $Zn_2SiO_4$. The emission band of the $ZnGa_2O_4$ electrode at about 700 nm may be attributed to luminescence from an oxygen defect in $ZnGa_2O_4$. Very weak emission is observed at about 370 nm. Similar emission is reported by Poort et al.[33] However, its origin is not clear at present. In the case of the $ZnGa_2O_4$ : Mn electrode, very strong emission at about 500 nm was observed. Although the emission peak is very similar to that of $ZnGa_2O_4$ under anodic bias, the emission center was considered to be $Mn^{2+}$ because of the very strong emission intensity.[9]

In order to investigate the effect of a reducing agent, $K_4[Fe(CN)_6]$ was added to $Na_2SO_4$ electrolyte solution. Figure 8 shows the $K_4[Fe(CN)_6]$ concentration dependence of the electrochemical luminescence intensity by the $ZnGa_2O_4$ electrode at 4 mA cm$^{-2}$. The addition of $K_4[Fe(CN)_6]$ hardly affected the electrochemical luminescence spectra and the breakdown voltage of the $ZnGa_2O_4$ electrode. The luminescence intensity was increased by the addition of $K_4[Fe(CN)_6]$. The luminescence intensity remained almost constant at a $K_4[Fe(CN)_6]$ concentration$\leq$0.01 M. However, it increased at a concentration$\geq$0.01 M. This result suggests that electrons are injected to the conduction band of $ZnGa_2O_4$ from $K_4[Fe(CN)_6]$ at large concentration. Bard et al. observed an anodic current by using several redox agents for the n-$TiO_2$ electrode.[15] They ascribed the anodic current to electron transfer from the occupied level of the redox species to the conduction band of $TiO_2$. Since the redox potential of $K_4[Fe(CN)_6]$ is more negative by 0.9 V than that of water, electrons are injected from $K_4[Fe(CN)_6]$ to the conduction band of the $ZnGa_2O_4$ more easily than from water molecules. This may be the reason why the addition of $K_4[Fe(CN)_6]$ increases the electrochemical luminescence intensity of the $ZnGa_2O_4$ electrode under anodic polarization.

The electrochemical luminescence intensity of the $ZnGa_2O_4$ electrode under anodic polarization was also measured by adding KI and KBr as reducing agents. Although the emission spectra and breakdown voltage were hardly influenced by adding KI and KBr, the intensity increased by the addition. Figure 9 shows the luminescence intensity at 4 mA cm$^{-2}$ against the redox potential of each reducing agent. The luminescence intensity increased with decreasing the redox potential. This result suggests that electrons for the impact excitation of luminescence centers in $ZnGa_2O_4$ are injected from the reducing agent on the electrode surface. These emissions were observed by imposing anodic bias at about +12.5 V, even in the presence of each reducing agent. Although anodic current was not obtained below +12.0 V because of the rectification of the n-type semiconductor, the current was caused by avalanche breakdown at +12.5 V.

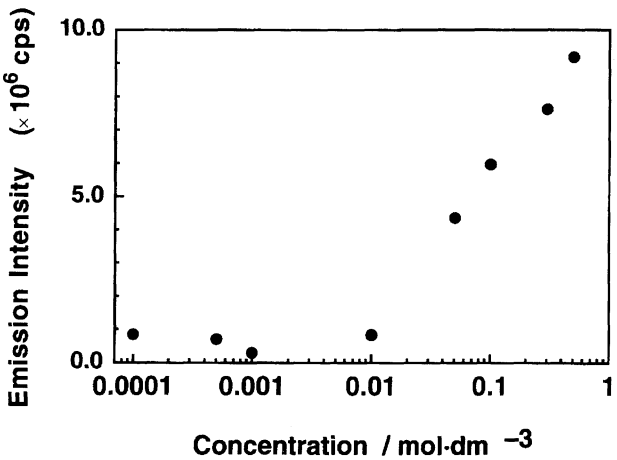


Fig. 8. Relation between emission intensity at 503 nm and $K_4[Fe(CN)_6]$ concentration at 4 mA cm$^{-2}$.

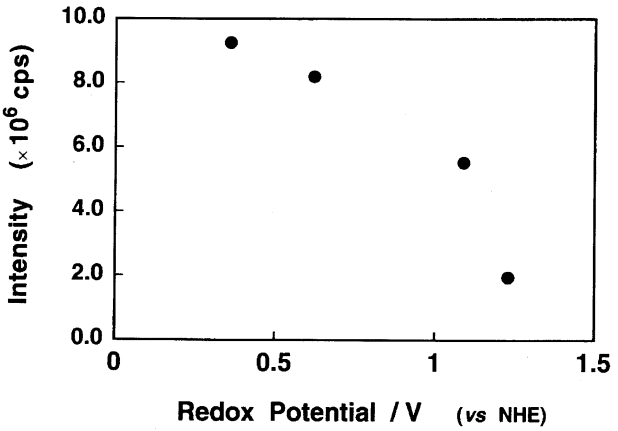


Fig. 9. Relation between emission intensity at 503 nm and redox potential at 4 mA $cm^{-2}$ in 0.5 M each reducing agent +0.5 M $Na_2SO_4$ electrolyte. Reducing agent: $K_4[Fe(CN)_6]$, KI, and KBr.

In order to clarify the injection mechanism, the temperature dependence of the luminescence intensity in the presence of a reducing agent was studied. Figure 10 shows the temperature dependence of the electrochemical luminescence of $ZnGa_2O_4$ in the presence of $K_4[Fe(CN)_6]$, KBr, and $Na_2SO_4$. The luminescence intensity hardly depends on temperature for each reducing agent. This result indicates that electron injection to the conduction band of the $ZnGa_2O_4$ electrode occurs equi-energetically without any activation energy.

Figure 11 illustrates schematically the mechanism of the electrochemical luminescence of the $ZnGa_2O_4$ electrode under anodic polarization. The flat band potential of the $ZnGa_2O_4$ electrode is estimated to be about −0.8 V vs. NHE (Normal Hydrogen Electrode) from the current–potential curve. When the $ZnGa_2O_4$ electrode is polarized strongly to about +12.5 V, avalanche breakdown occurs at the depletion layer where electrons are injected from the reducing agent equi-energetically. Injected electrons are accelerated at a strong electric field in the depletion layer and obtain kinetic energy to excite the luminescence centers in the $ZnGa_2O_4$ electrode by impact.

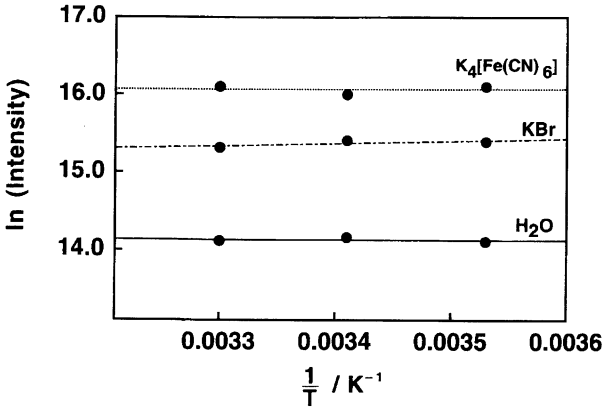


Fig. 10. Arrhenius plots of emission intensity at 503 nm in 0.5 M $Na_2SO_4$ electrolyte and adding 0.5 M $K_4[Fe(CN)_6]$ or 0.5 M KBr.

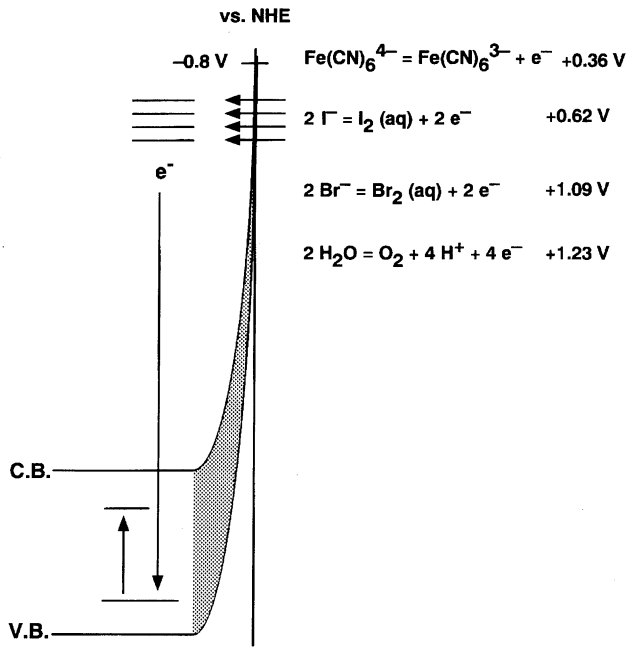


Fig. 11. A schematic mechanism of electrochemical luminescence under anodic polarization in the presence of reducing agent.

## References

1 K. Akagi, H. Kukimoto, and T. Nakayama, *J. Lumin.*, **17**, 237 (1978).

2 S. Oda, K. Akagi, H. Kukimoto, and T. Nakayama, *J. Lumin.*, **16**, 323 (1978).

3 H. Kukimoto, S. Oda, and T. Nakayama, *J. Lumin.*, **18/19**, 365 (1979).

4 L. E. Shea, R. K. Datta, and J. J. Brown, Jr., *J. Electrochem. Soc.*, **141**, 2198 (1994).

5 S. Itoh, H. Toki, Y. Sato, K. Morimoto, and T. Kishino, *J. Electrochem. Soc.*, **138**, 1509 (1991).

6 S. Itoh, T. Kimizuka, and T. Tonegawa, *J. Electrochem. Soc.*, **136**, 1819 (1989).

7 S. Itoh, M. Yokoyama, and K. Morimoto, *J. Vac. Sci. Technol.*, **A5**, 3430 (1987).

8 C. W. W. Hoffman and J. J. Brown, *J. Inorg. Nucl. Chem.*, **30**, 63 (1968).

9 L. E. Shea, R. K. Datta, and J. J. Brown, Jr., *J. Electrochem. Soc.*, **141**, 1950 (1994).

10 C. F. Yu and P. Lin, *J. Appl. Phys.*, **79**, 7191 (1996).

11 T. K. Tran, W. Park, J. W. Tomm, B. K. Wagner, S. M. Jacobsen, C. J. Summers, P. N. Yocom, and S. K. McClelland, *J. Appl. Phys.*, **78**, 5691 (1995).

12 J. J. Brown, *J. Electrochem. Soc.*, **114**, 245 (1967).

13 F. C. Romeijn, *Philips Res. Rep.*, **8**, 304 (1953).

14 R. K. Datta and R. Roy, *J. Am. Cer. Soc.*, **50**, 578 (1967).

15 R. N. Noufi, P. A. Kohl, S. N. Frank, and A. J. Bard, *J. Electrochem. Soc.*, **125**, 246 (1978).

16 T. Ohtake, N. Sonoyama, and T. Sakata, *Chem. Phys. Lett.*, **298**, 395 (1998).

17 I. J. Hsieh, M. S. Feng, K. T. Kuo, and P. Lin, *J. Electrochem. Soc.*, **141**, 1617 (1994).

18 I. J. Hsieh, K. T. Chu, C. F. Yu, and M. S. Feng, *J. Appl.*

*Phys.*, **76**, 3735 (1994).
19 Y. Nakato, A. Tsumura, and H. Tsubomura, *Chem. Phys. Lett.*, **85**, 387 (1982).
20 Y. Nakato, A. Tsumura, and H. Tsubomura, *J. Phys. Chem.*, **87**, 2402 (1983).
21 Y. Nakato, H. Ogawa, K. Morita, and H. Tsubomura, *J. Phys. Chem.*, **90**, 6210 (1986).
22 G. Nogami, Y. Ogawa, and Y. Nishiyama, *J. Electrochem. Soc.*, **135**, 3008 (1988).
23 R. Memming, *J. Electrochem. Soc.*, **116**, 785 (1969).
24 H. Morisaki and K. Yazawa, *Appl. Phys. Lett.*, **33**, 1013 (1978).
25 D. Fichou and J. Kossanyi, *Chem. Lett.*, **1985**, 1205.
26 J. C. Tranchart, L. Hollan, and R. Memming, *J. Electrochem. Soc.*, **125**, 1185 (1978).
27 G. C. Wood and C. Pearson, *Corros. Sci.*, **7**, 119 (1967).
28 J. Gautron, J. -P. Dalbéra, and P. Lemasson, *Surf. Sci.*, **99**, 300 (1980).
29 P. Lemasson, J. Gautron, and J. -P. Dalbéra, *Ber. Bunsenges. Phys. Chem.*, **84**, 796 (1980).
30 K. Takahashi, "Semiconductor Engineering," Morikita Press Inc., p. 111 (1993).
31 G. Petermann, H. Tributsch, and R. Bogomolni, *J. Chem. Phys.*, **57**, 1026 (1972).
32 C. Barthou, J. Benoit, P. Benalloul, and A. Morell, *J. Electrochem. Soc.*, **141**, 524 (1994).
33 S. H. M. Poort, D. Cetin, A. Meijerink, and G. Blasse, *J. Electrochem. Soc.*, **144**, 2179 (1997).